Zoology 124 (2017) 106–118

Contents lists available at ScienceDirect

Zoology

journal homepage: www.elsevier.com/locate/zool

Functional correlates of the position of the axis of rotation of the mandible during chewing in non-human primates☆

Jose Iriarte-Diaz[a,*], Claire E. Terhune[b], Andrea B. Taylor[c], Callum F. Ross[d]

[a] Department of Oral Biology, University of Illinois at Chicago, 801 S. Paulina St., Chicago, IL 60612, USA
[b] Department of Anthropology, University of Arkansas, Fayetteville, AR 72701, USA
[c] Department of Basic Science, Touro University, Vallejo, CA 94592, USA
[d] Department of Organismal Biology and Anatomy, The University of Chicago, Chicago, IL 60637, USA

ARTICLE INFO

Keywords:
Primates
Feeding kinematics
Chewing
Helical axis

ABSTRACT

The location of the axis of rotation (AoR) of the mandible was quantified using the helical axis (HA) in eight individuals from three species of non-human primates: *Papio anubis*, *Cebus apella*, and *Macaca mulatta*. These data were used to test three hypotheses regarding the functional significance of anteroposterior condylar translation − an AoR located inferior to the temporomandibular joint (TMJ) − during chewing: minimizing impingement of the gonial region on cervical soft tissue structures during jaw opening; avoiding stretching of the inferior alveolar neurovascular bundle (IANB); and increasing jaw-elevator muscle torques. The results reveal that the HA is located near the occlusal plane in *Papio* and *Cebus*, but closer to the condyle in *Macaca*; is located anteroinferior to the TMJ during both opening and closing in *Papio*, as well as during opening in *Macaca* and *Cebus;* and varies in its location during closing in *Macaca* and *Cebus*. The impingement hypothesis is not supported by interspecific variation in HA location: species with larger gonial angles like *Cebus* do not have more inferiorly located HAs than species with more obtuse mandibular angles like *Papio*. However, intraspecific variation provides some support for the impingement hypothesis. The HA seldom passes near or through the lingula, falsifying the hypothesis that its location is determined by the sphenomandibular ligament, and the magnitudes of strain associated with a HA at the TMJ would not be large enough to cause problematic stretching of the IANB. HA location does affect muscle moment arms about the TMJ, with implications for the torque generation capability of the jaw-elevator muscles. In *Cebus*, a HA farther away from the TMJ is associated with larger jaw-elevator muscle moment arms about the joint than if it were at the TMJ. The effects of HA location on muscle strain and muscle moment arms are largest at large gapes and smallest at low gapes, suggesting that if HA location is of functional significance for primate feeding system performance, it is more likely to be in relation to large gape feeding behaviors than chewing. Its presence in humans is most parsimoniously interpreted as a primitive retention from non-human primate ancestors and explanations for the presence of anteroposterior condylar translation in humans need not invoke either the uniqueness of human speech or upright posture.

1. Introduction

The location and orientation of the axis of rotation (AoR) of a joint can have profound consequences for musculoskeletal function (Van den Bogert et al., 2008; Beyer et al., 2015). This is especially true for the AoR of the mandible, which varies across mammals from a fixed location within the temporomandibular joint (TMJ) of some carnivores to the moving rotational axis in pigs (Keefe et al., 2008, 2009; Menegaz et al., 2015) and human and non-human primates (Gallo et al., 1997, 2000, 2006; Terhune et al., 2011). Ideas regarding the functional significance of mandibular AoR location have often been expressed as hypotheses regarding the functional significance of anteroposterior translation of the mandibular condyle in the TMJ, sometimes called 'sagittal sliding' (Hiiemäe and Kay, 1973; Smith, 1985; Wall, 1999; Hylander, 2006). This focus on condylar translation is attributable to the large magnitude of anteroposterior condylar translation in humans, its relevance for the etiology of disk derangements in human temporomandibular disorders (e.g., Farrar, 1978; Katzberg et al., 1982), and the fact that it is easier to measure condylar displacement than AoR location. However, because anteroposterior condylar displacement during chewing is often − depending on species − accompanied by significant superorinferior displacement, hypotheses regarding

☆ This article is part of a special issue entitled 'Determinants of Mammalian Feeding System Design'.

* Corresponding author.
E-mail address: jiriarte@uic.edu (J. Iriarte-Diaz).

http://dx.doi.org/10.1016/j.zool.2017.08.006
Received 11 May 2017; Received in revised form 16 August 2017; Accepted 16 August 2017
Available online 23 August 2017
0944-2006/

condylar movements are better expressed as hypotheses regarding the location of AoR (Weijs et al., 1989; Gallo et al., 2000). Moreover, recent advances in motion capture and XROMM technology have made estimation of AoR location significantly easier.

The biological significance of variation in the AoR of the primate mandible lies in the consideration of what it means for movements of the mandibular condyles, muscle attachments, and teeth, as well as for strain of muscles and neurovascular bundles. The present paper uses data on the location and orientation of the mandibular AoR in three species of non-human primates to test hypotheses regarding the functional significance of AoR position. As early as 1908 it was recognized that the center of rotation (CoR), which is the estimated AoR from 2D data, is often located posterior and inferior to the condyle; this is associated with anteroposterior and superoinferior translation of the mandibular condyle (Bennett, 1908; Grant, 1973a,b; Weijs et al., 1989).

Smith (1985) reviewed and evaluated three plausible functional hypotheses for "condylar translation" in humans: (i) the airway/carotid sheath *impingement hypothesis* (Smith, 1985), (ii) the *neurovascular strain hypothesis* (Moss, 1960, 1975, 1983), and (3) the sarcomere stretch, or, as we prefer to call it, the *jaw-elevator torque generation hypothesis* (Carlson, 1977; Hylander, 1978). The present paper evaluates the relative importance of these factors for interspecific feeding system design in primates.

1.1. The impingement hypothesis

The impingement hypothesis postulates that a posterior and inferior location for the mandibular AoR allows mandibular depression to occur without the mylohyoid muscle and hyoid bone impinging on the airway and esophagus, and without the gonial angles of the mandible impinging on the carotid sheaths or other soft tissue structures in the neck. It has been argued that this is especially necessary in humans because of the unusual position of the larynx associated with speech, the pharynx associated with upright posture, and the mandibular condyle high above the occlusal plane (Smith, 1985). The present paper focuses on the more general question of whether impingement on cervical soft tissues is a morphological constraint in the evolution of the primate feeding system. Specifically, we evaluate whether, in interspecific comparisons, there is a relationship between the position of the AoR and the degree to which the mandibular gonial angle protrudes posterior to the mandibular condyle. The impingement hypothesis predicts that the more the gonial angle protrudes behind the TMJ, the lower the AoR is in order to minimize posterior displacement of the gonial region during jaw opening. Additionally, the amount of posterior displacement a mandible incurs depends on gape angle, with larger gape angles more likely to impinge on cervical structures. Consequently, if the impingement hypothesis is correct, we predict that species and individuals with more posteriorly protruded gonial angles will have greater inferior AoR, and that the AoR location will be correlated with gape angle.

1.2. The neurovascular strain hypothesis

This hypothesis posits that the AoR should be located near the mandibular foramen to prevent overstretching of the inferior alveolar neurovascular bundle (IANB) during jaw opening, and that the attachment of the sphenomandibular ligament to the lingula is the mechanism whereby this location of the AoR is produced (Moss, 1960, 1975, 1983). The rationale behind this hypothesis is that cyclical stretching of the IANB could produce structural and functional damage to the nerve, hence an AoR that minimizes this strain should be selected. Nerve conduction experiments have shown that strains of 5% can temporarily decrease nerve conduction and that strains of 10–15% or more can have permanent effects (Li and Shi, 2007; Rickett et al., 2011). Here we quantify the location of the mandibular AoR relative to the mandibular foramen and estimate the amount of strain that the IANB would experience if it ran directly from the foramen ovale to the mandibular foramen at minimum gape. We use these estimates of the AoR to test the above hypothesis that nerve strain reduction is an important determinant of mandibular kinematics in non-human primates.

1.3. The jaw-elevator torque hypothesis

The amount of torque that the jaw-elevator muscles can apply to bite force depends on their location and orientation relative to the jaw joint. The location of the AoR obviously has no bearing on the relative magnitudes of bite and joint reaction forces in static situations because the AoR does not exist (Stern, 1974; Hylander, 1975). However, AoR location *does* affect the relationship between gape distance – the distance between the upper and lower incisors – and both the moment arms of the jaw elevators and the regions of the length–tension curves on which these muscles operate, which in turn impacts the jaw-elevator muscle torques and the associated bite forces in static conditions, including isometric biting (Carlson, 1977; Weijs et al., 1989). The force-generating capacity of a muscle varies as a function of where on its length–tension curve it is operating, and the muscle's length at a given joint angle is determined by its location relative to the AoR: the further the line of action from the AoR, the larger will be the change in muscle length with any change in gape angle. The actual effect of changes in jaw-elevator muscle lengths on their force-generating capacity depends on the jaw gape angle at which they are at the peaks of their length–tension curves (Anapol and Herring, 1989; Weijs et al., 1989).

Carlson (1977) evaluated the impact of AoR location on jaw-elevator muscle torques in macaque monkeys, calculating the relationships between 'functional gape angle' and both masseter length and masseter moment arm with the AoR in its natural location – inferior and posterior to the TMJ – and through the TMJ. Carlson showed that, compared with an axis located at the TMJ, the inferoposterior location of the actual AoR reduces the amount the masseter moment arm decreases during jaw opening. In other words, by positioning the AoR closer to the posterior border of the masseter, decreases in the torque-generating capacity of the masseter associated with jaw opening are ameliorated. Carlson also found that the inferoposterior location of the AoR reduces the amount of sarcomere stretch associated with jaw depression. Assuming the masseter muscle sarcomeres were at their optimal length at centric occlusion, he argued that stretching the sarcomeres would reduce the force generation capacity of the muscles. Carlson (1977) estimated that the benefits due to reduced sarcomere stretch are greater than those due to reduced decreases in moment arms and called for similar analyses for other jaw-elevator muscles, which we provide here.

Carlson's conclusions were partially supported by a study that evaluated the effect of different locations of the mandibular AoR on the torque-generating capacity of the jaw-elevator muscles in rabbits (Weijs et al., 1989). In this study the authors argued that in many animals, including humans, optimal sarcomere length occurs at gapes larger than minimum gape, i.e., centric occlusion (Nordstrom et al., 1974; Nordstrom and Yemm, 1974; Thexton and Hiiemae, 1975; Anapol and Herring, 1989), so that some degree of jaw depression brings the masseter to the peak of its length–tension curve. Nonetheless, as in Carlson's study, Weijs et al. (1989) found the location of the AoR minimizes muscle stretch of both masseter and medial pterygoid, mitigating the reduction in active force generation. Furthermore, they measured the magnitude of passive elastic forces resisting jaw depression with the AoR in its normal position and compared it with estimates of these forces when the AoR was located at a range of different positions, both further from and closer to the TMJ. They concluded that the location of the AoR "is as low as necessary to minimize the passive forces in the jaw-closing muscles" while simultaneously allowing "maximal active forces to be generated over a large range of gapes" (Weijs et al., 1989, p. 145). In the present paper we quantify the impact of AoR location on lever arms and muscle lengths for the temporalis, masseter and medial pterygoid jaw elevators during chewing in three species of non-human primates.

2. Materials and methods

2.1. Experimental subjects

Three-dimensional (3D) jaw kinematics during feeding were recorded in one adult male and two adult female rhesus macaques (*Macaca mulatta*), three adult female tufted capuchins (*Sapajus* (*Cebus*) *apella*), and two adult female baboons (*Papio anubis*). Animals were housed and studied at the University of Chicago in accordance with Federal regulations and approved IACUC protocols.

2.2. Data collection

Kinematic data were collected using 3D motion capture methods described in detail elsewhere (Reed and Ross, 2010). Briefly, at least three reflective markers were coupled to each of the mandible and cranium using permanently implanted percutaneous bone screws and their movements recorded in 3D using a ten camera Vicon system at either 100 or 250 frames s^{-1}. Animals were trained to feed in front of the cameras following previously published protocols (Reed and Ross, 2010; Iriarte-Diaz et al., 2011). Data presented here represent rhythmic chewing cycles while animals fed on grapes, apples, sweet potatoes, dry fruits, and a variety of nuts. A total of 7320 chewing cycles was analyzed (see Table 1 for a more detailed description). After the recording sessions, the animals' heads, with the screws in place, were CT scanned at the University of Chicago Medical Center using a Phillips Brilliance Big Bore CT scanner at 120 kVp and 263 mA. Scans had a slice thickness of 0.8 mm and an inter-slice separation of 0.4 mm. Amira 5.4.2 (Visage Imaging, Inc., San Diego, CA, USA) was used to create polygonal mesh surface models of the bones and markers from these scans, from which the position of the markers relative to the mandible and cranium were calculated.

2.3. Data processing

Vicon data were imported into MATLAB for processing. The 3D movement data were filtered with a fourth-order, low-pass Butterworth filter with a 15-Hz cutoff frequency. The 3D movement of the mandibular markers was calculated in a local coordinate system fixed to the cranium: the origin of the coordinate system was placed between the two condyles, the Y-axis passing across the tops of the mandibular condyles (positive to the left), the X-axis running towards the front of the cranium with the XY-plane parallel with the occlusal plane (Fig. 1A), and the Z-axis orthogonal to this plane (positive upwards). The 'reference position' is the location of the mandibular markers with the mandible in centric occlusion. Rigid-body kinematics of the mandible were calculated by finding the 4x4 homogenous transformation matrices (**T**) between the set of mandibular markers at each time step with respect to the reference position by singular value decomposition methods (Söderkvist and Wedin, 1993) using the KineMat toolbox in MATLAB (Reinschmidt and van den Bogert, 1997). These transformation matrices are composed of both a 3x3 rotation matrix (**R**) and a 3x1 translation matrix (**t**) as

$$\mathbf{T} = \begin{bmatrix} \mathbf{R} & \mathbf{t} \\ 0\,0\,0 & 1 \end{bmatrix}.$$

The rigid-body motion of the mandible was described using the instantaneous helical axis (IHA) method, in which the relative movement between two rigid bodies is characterized by the translation velocity along, and a rotation velocity around, a moving axis, the IHA. In this method, the IHA parameters to be estimated are the position (**p**) and direction (**n**) of the moving helical axis, as well as the angular velocity around (ω) and the linear velocity (v) along the IHA. These parameters are derived from the rotation component (**R**) of the homogenous transformation matrix and its derivative ($\dot{\mathbf{R}}$) as follows:

$$\frac{1}{2}[\dot{\mathbf{R}}\mathbf{R}^{\mathrm{T}} - \mathbf{R}\dot{\mathbf{R}}^{\mathrm{T}}] = \begin{bmatrix} 0 & -\omega_z & \omega_y \\ \omega_z & 0 & -\omega_x \\ -\omega_y & \omega_x & 0 \end{bmatrix},$$

$$\boldsymbol{\omega} = \begin{bmatrix} \omega_x \\ \omega_y \\ \omega_z \end{bmatrix},$$

where $\boldsymbol{\omega}$ is the angular velocity vector, and ω_i is the magnitude of the angular velocities in the i-th directions. Once the angular velocity vector is estimated, the angular velocity around the IHA (ω) is estimated by

$$\omega = ||\,\boldsymbol{\omega}\,||,$$

$$\mathbf{n} = \frac{\omega}{||\,\boldsymbol{\omega}\,||},$$

$$v = \mathbf{n}^T\dot{\mathbf{t}},$$

$$\mathrm{p} = \mathrm{t} + \frac{\omega \times \dot{\mathbf{t}}}{\omega^2}.$$

Since IHA becomes ill-defined when ω approaches zero, only data where $\omega > 10$ degrees/sec were considered.

In addition to documenting changes in the location and orientation of the HA throughout the gape cycle, we focused on the time step at which the HA angular velocity (ω) reached a maximum value (HA_{maxRot}, Fig. 1B) during the opening and closing phases in each gape cycle. Following Gallo and colleagues (Gallo et al., 1997, 2000), the location of the HA was reported as the intersections of the helical axis with the parasagittal planes passing through the balancing and working side condyles (p_{BS} and p_{WS}, respectively) (Fig. 1B).

The rigid-body kinematics of the mandible were also described using Euler/Cardan angles (with Y-Z-X order sequence) with respect to the reference position (i.e., centric relation), using the KineMat toolbox. Rotation around the Y-axis describes mostly jaw opening and closing. Starting from occlusion at minimum gape, rotation around the Y-axis increases to maximum gape, and rotation decreases during the jaw closing phase. Using Y-axis rotation, feeding sequences were divided into discrete gape cycles by identifying the local minimum corresponding to consecutive minimum gapes. Gape cycles were time-standardized by interpolating each cycle into 100 time steps. Individual cycles were identified as left or right chews using the rotation around the Z-axis as the jaw approached minimum gape. During a chewing cycle, the mandible moves towards the working side (i.e., the chewing side) during the opening phase, and then towards the balancing side during the closing phase. Thus, right chews are defined as those cycles in which the mandible was moving towards the left side at the end of the gape cycle (i.e., with positive angular velocity around the Z-axis), and left chews when the mandible was moving towards the right side. To compare the kinematics during both events, we combined both left and right chews as working and balancing sides. Effectively, we mirrored all left chew kinematics so all analyzed chews represent right

Table 1
Number of analyzed gape cycles per individual.

Species	Individual	Number of cycles	
		Right	Left
Papio (baboon)	B1	405	410
	B2	160	342
Cebus (capuchin)	C1	634	811
	C2	637	506
	C3	511	821
Macaca (macaque)	M1	214	343
	M2	100	143
	M3	1063	220

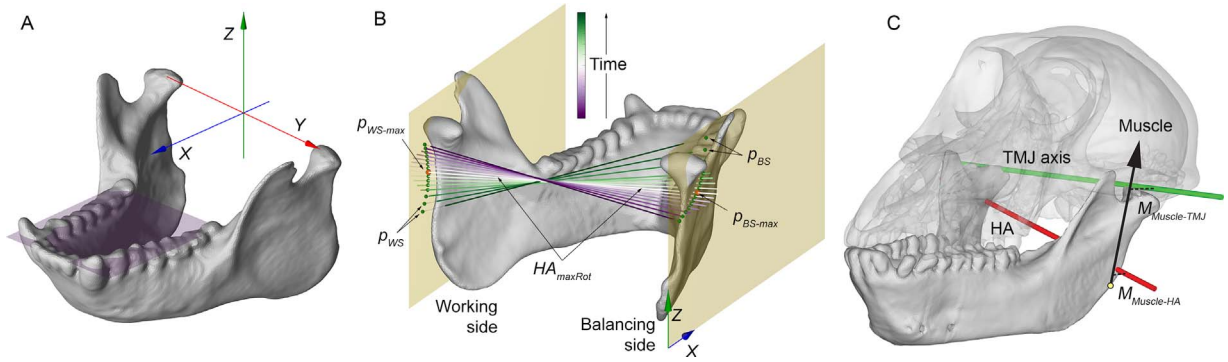

Fig. 1. Diagram of axes and parameters. (A) Mandible depicting the local coordinate system used in this study. The purple-shaded plane indicates the occlusal plane used to orient the X–Y plane. (B) Instantaneous helical axis (HA) locations during the opening phase of a gape cycle. HA locations at different time steps are color-coded from purple (close to minimum gape) to green (close to maximum gape). Beige parasagittal planes correspond to the condylar planes passing through the balancing- and working-side condyles. Green circles indicate the intersection of each HA with the condylar planes (p_{WS} and p_{BS} for the working and balancing sides, respectively). The amount of instantaneous rotation around each HA is represented by the length of the axis. The HA with the highest instantaneous rotation (HA_{maxRot}) is indicated by the white axis, and its intersections with the condylar planes are indicated by the red circles on both working and balancing sides ($p_{WS\text{-}max}$ and $p_{BS\text{-}max}$, respectively). (C) Diagram indicating the calculation of the moment arms around the moving helical axis (HA) and the TMJ axis (the axis representing the theoretical condition of the mandible moving with a hinge joint at the TMJ). The line of action of the muscle (in this case, the masseter) is represented by the black arrow, the TMJ axis is represented by the green cylinder, and the HA is represented by the red cylinder. The minimum perpendicular distances between the muscle line of action and the HA and the TMJ axis, indicated by dashed lines, represent the moment arms $M_{Muscle\text{-}HA}$ and $M_{Muscle\text{-}TMJ}$, respectively.

chews only.

2.4. Effect of gape angle on HA position

Because maximum gape angle is expected to be different within and between individuals, the relationship between maximum gape angle and the horizontal and vertical position of the HA_{maxRot} was estimated using correlation analysis for each individual. For each analyzed gape cycle, the maximum gape angle was represented by the maximum value of the Euler angle around the Y-axis, and the HA_{maxRot} was estimated as the mean value between $p_{BS\text{-}max}$ and $p_{WS\text{-}max}$ (i.e., the position of the HA_{maxRot} as it crosses the sagittal plane), for both opening and closing phases of the gape cycle. Due to the large sample sizes in our sample, low correlations with little biological significance may still be statistically significant. Because of this, we considered only correlations above a threshold of 0.3 in our results and discussion as "biologically relevant". Thus, it could be possible to have a statistically significant but not biologically relevant correlation (i.e., $p < 0.05$ and $r < 0.3$). This threshold is not strict and could be changed, but is a starting point for evaluating the relative contribution of gape angle to jaw mechanics.

2.5. Simulating mandible movement without translation

To evaluate the effect of having a HA that is *not* located near the TMJ axis, we simulated a theoretical kinematic condition of only mandible rotation around the origin without mandible translation. This simulated condition, henceforth called the 'hinge-joint condition', uses only the calculated rotation matrices **R** for each individual and sets their translation matrices **t** to zero. This effectively simulates the mandible movement as if the axis of rotation is located close to the TMJ axis, that is, that the mandible only rotates around the X-, Y-, and Z-axes of the coordinate system without overall translation of the mandible as a whole (Fig. 2). It is worth noting that this simulated hinge-joint condition is not a true hinge joint, which is defined as having only rotations around its Y-axis. Our simulation allows for rotations around the X- and Z-axes, although these rotations tend to be small, so that we consider the system as a quasi-hinge joint. As such, different physiological parameters (see Sections 2.7 and 2.8) were calculated for both the experimentally observed kinematics and for the simulated, hinge-joint condition. The comparison between the values from these two conditions will provide information on the effect of having a HA that is *not* the TMJ axis.

2.6. Testing the impingement hypothesis

The impingement hypothesis predicts that the more the gonial angle protrudes behind the TMJ, the lower the AoR must be in order to minimize posterior displacement of the gonial region during jaw opening. For each individual, mean vertical position of the intersection of the HA with the sagittal plane at maximum angular velocity, HA_{vert}, was calculated for both opening and closing phases and plotted against the horizontal position of the gonial angle, GA_{horiz}. The GA_{horiz} was measured directly from the mandible 3D models in lateral view, as the horizontal distance from the gonial angle to the vertical line that passes through the mandibular condyle (see Fig. 6A). Non-parametric correlations were performed for all individuals using Spearman's r statistic with $\alpha = 0.05$. All distances were calculated as % of jaw length to compare species of different size.

2.7. Testing the neurovascular strain hypothesis

To evaluate the neurovascular strain hypothesis, the potential strain of the inferior alveolar neurovascular bundle (IANB) was estimated throughout the gape cycle. Strain was estimated by calculating the distance between the foramen ovale and the mandibular foramen (inter-foramina distance, IFD), expressed as a percentage of length change with respect to the IFD at centric occlusion, henceforth referred to as the 'reference position'. If this hypothesis were correct, we would expect strain in the IFD to fall below a threshold value that would affect conduction physiology of the nerve. In this case, we assume this value to be 5% following findings from previous studies from isolated nerve preparations (e.g., Rickett et al., 2011). Additionally, we would expect to see a reduction in strain when comparing the maximum strain observed experimentally with the strain expected in the simulated, theoretical condition.

2.8. Testing the jaw-elevator torque hypothesis

To evaluate the effects of changes in mandible position through the gape cycle on the torque- generating capacity of the masticatory muscles, muscle fiber strain and moment arms of three different segments of each jaw-elevator muscle were calculated about both the dynamic HA and the "theoretical" TMJ axis, i.e., the axis connecting the top of the mandibular condyles at centric occlusion.

Muscle strain was estimated by calculating the changes in total muscle length, i.e., the distance between the mandibular and cranial

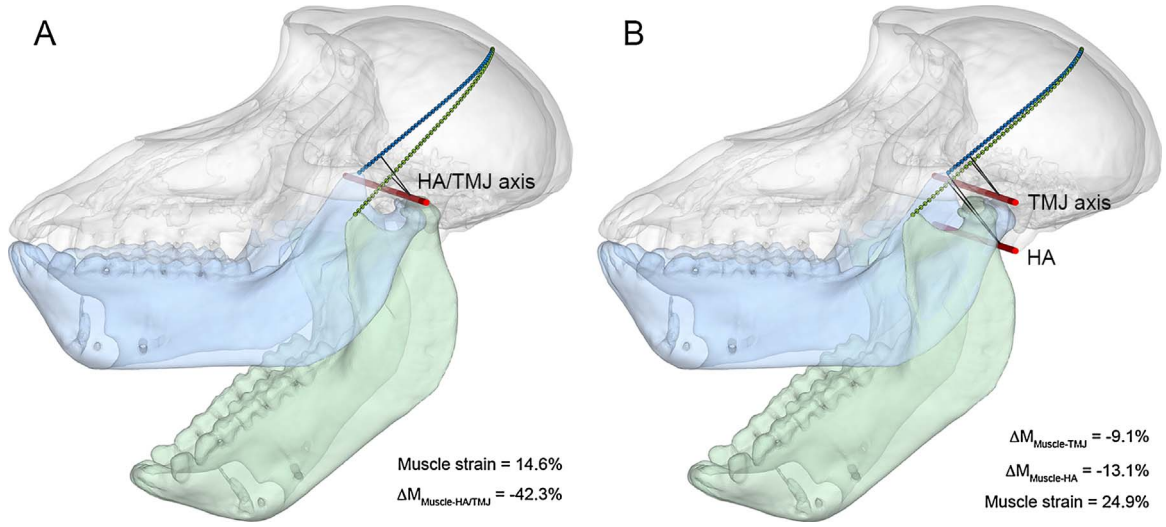

Fig. 2. Example of the effect of simulated HA locations on the muscle strain and muscle moment arm for a temporalis segment. The blue and green mandibles represent the mandibles during centric occlusion and during maximum gape, respectively. The blue symbols represent the position of the middle segment of the temporalis muscle during centric occlusion and the green symbols represent the muscle segment at maximum gape. Black lines represent the moment arms of the muscle segments to specific rotation axes. Muscle strains are calculated as the percentage of change in muscle length from occlusion to maximum gape. The difference in muscle moment arm to the TMJ axis and HA ($\Delta M_{Muscle\text{-}TMJ}$ or $\Delta M_{Muscle\text{-}HA}$, respectively), is calculated as the percentage difference in moment from occlusion to maximum gape. (A) Simulated condition where the mandible is rotated 40 degrees around the TMJ axis, without mandible translation. In this case, the TMJ axis is the same as the helical axis (HA). (B) The mandible is rotated 40 degrees around the TMJ axis and then translated 10 mm forward. In this case, the HA is located below and anterior to the TMJ axis, representing a more realistic mandible movement.

attachments of each muscle segment, expressed as a percentage of the length of the muscle at the reference position. The lines of action of individual muscle fibers were calculated for the anterior, middle, and posterior segments of the three major masticatory muscles: temporalis, superficial masseter, and medial pterygoid muscles (see Fig. S1 in the supplementary online Appendix). The muscle fibers for both the masseter and the medial pterygoid were modeled as straight lines between the cranial and mandibular attachments. For the temporalis, however, the muscle fibers wrap over the cranial surface, so a line of action was calculated from the line connecting the mandibular attachment to the tangential point on the cranial surface. To calculate the total muscle length of the temporalis, each fiber was divided into 20 equidistant segments wrapping over the cranial surface, and the distance between consecutive points was added together. The muscle moment arms for each muscle segment were calculated around both the varying HA ($M_{Muscle\text{-}HA}$) and the fixed TMJ axis ($M_{Muscle\text{-}TMJ}$) as

$$M_{Muscle-Axis} = (\mathbf{d}_{Muscle-Axis} \times \mathbf{n}_{Muscle}) \cdot \mathbf{n}_{Axis},$$

where $\mathbf{d}_{Muscle\text{-}Axis}$ is the distance vector between the muscle mandibular attachment and a point along the specific axis, $\mathbf{n}_{Muscle}$ is the direction of the line of action of the muscle segment, and $\mathbf{n}_{Axis}$ is the direction of the specific axis about which the moment is calculated (Fig. 1C). Moment arms are reported as a percentage of that individual's jaw length, to facilitate comparison of species of disparate size. These calculations were made in 3D for every time step and for every experimental feeding sequence recorded.

3. Results

3.1. Variation within and between species

The location of the HA at maximum rotation velocity (HA_{maxRot}) during opening and closing phases is depicted by $p_{WS\text{-}max}$ and $p_{BS\text{-}max}$ – the mean positions of the HA intersections with the parasagittal planes passing through working- and balancing-side condyles, respectively (Fig. 3). The overall rigid-body kinematics of the mandible are represented by the Euler/Cardan rotations around the X-, Y-, and Z-axis, through a mean gape cycle, from minimum gape to maximum gape, then back to minimum gape (insets in Fig. 3). In most individuals the mean location of the HA is more posterior during closing (blue symbols) than during opening (red symbols in Fig. 3). In addition, during closing $p_{BS\text{-}max}$ tends to be inferior and posterior to $p_{WS\text{-}max}$, whereas during opening $p_{WS\text{-}max}$ and $p_{BS\text{-}max}$ are more similar. Differences in the location of $p_{WS\text{-}max}$ and $p_{BS\text{-}max}$ indicate a HA that is not parallel with the TMJ axis, so these results indicate that the jaw shows less transverse movement during opening than during closing.

Inter-specific differences are apparent. In baboons, the HA is located anterior to the articular condyle, near or below the occlusal plane. In macaques, the HA is located either anterior (in M2 and M3) or below the articular condyle (in M1), and between the articular condyle and the occlusal plane. In capuchins, the HA is below (or slightly in front) of the articular condyle, but its vertical location varies among individuals, from above (in C1), at (in C2) or below the occlusal plane (in C3).

It is important to note that Fig. 3 shows the HA location at only one specific moment during each of the closing and opening phases of the gape cycle, whereas in reality the direction and location of the HA changes continuously through the cycle. In Fig. 4 the mean HA throughout the gape cycle during right chews is plotted for each subject. In all individuals the HA is more horizontal (i.e., closer to parallel with the condylar axis) at the end of closing and start of opening. During the opening phase, the HA moves first anterior and then backwards and superior, while during the closing phase, the HA moves upwards, towards the condyle. In addition, the HA of the working (i.e., right) side shows less variation than that of the balancing (i.e., left) side (Fig. 4). Species-specific differences are most notable during the opening phase. In baboons, changes in HA position are associated with small changes in orientation, and in macaques the changes in direction are slightly greater, but are still subtle. In contrast, in capuchins, during the opening phase the HA shows much larger changes in HA direction than in the two other species (Fig. 4).

The horizontal and vertical position of the HA_{maxRot} also varies with maximum gape angle but the relationship depends on the species and the individuals (Table 2 and Fig. 5). Almost all individuals (with the exception of the individuals B2 and M2) showed a statistically significant correlation (i.e., $p < 0.05$) between the position of the HA_{maxRot} and the gape angle for both opening and closing positions. However, not all of these statistically significant correlations are also "biologically relevant" (i.e., $r > 0.3$). *Papio* showed no biologically relevant

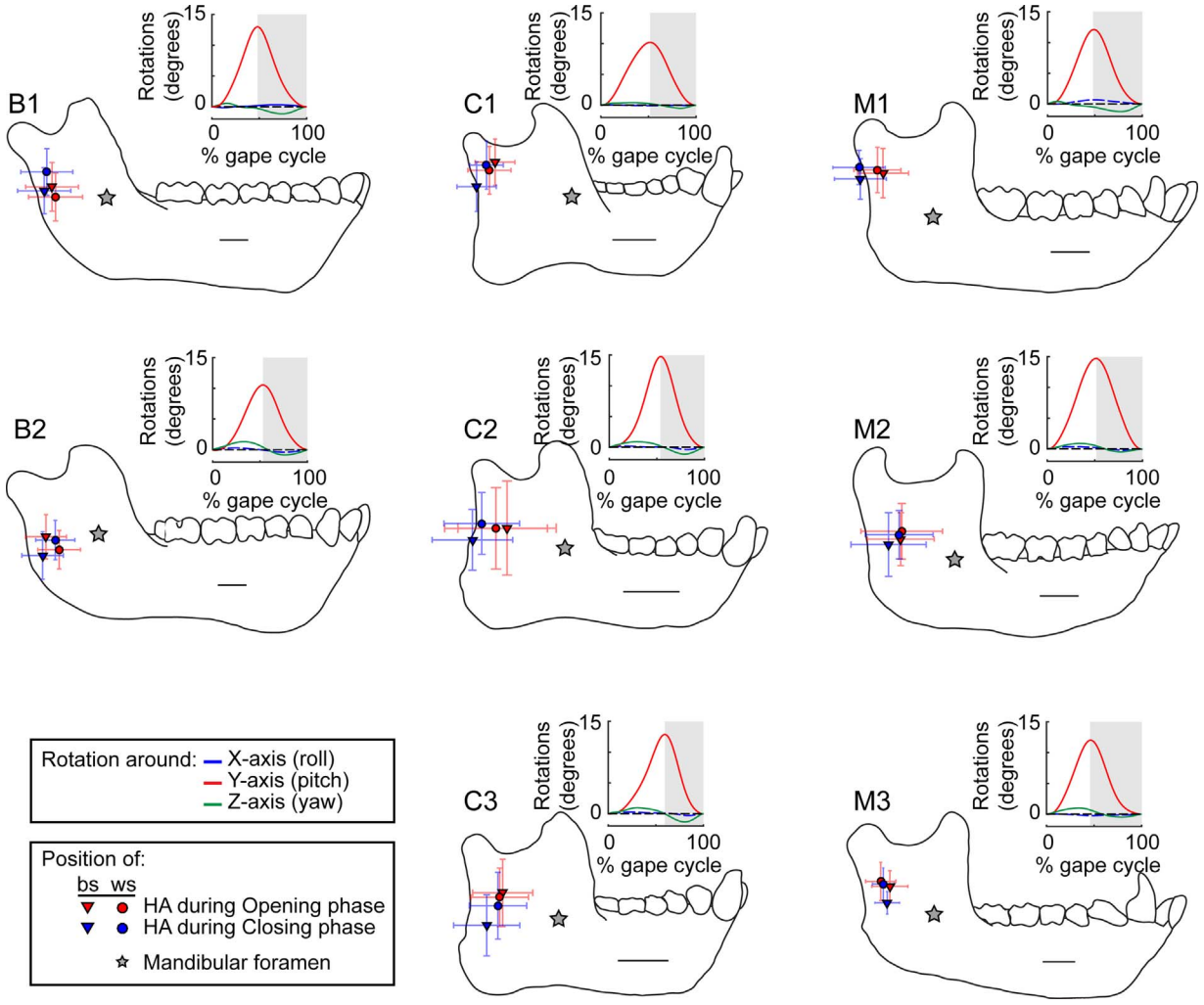

Fig. 3. Mean location of the helical axis (HA) at maximum angular velocity (HA_{maxRot}) in two baboons (B1, B2), three capuchins (C1, C2, C3), and three macaques (M1, M2, M3). The mandible geometry is based on CT scans of the individual subjects, the horizontal line in each mandible represents a 1 cm scale. The grey star represents the location of the mandibular foramen in each individual, which was used to evaluate the neurovascular strain hypothesis (see Fig. 5). Circles and triangles indicate the intersections of the HA with parasagittal planes passing through the balancing- ($p_{BS\text{-}max}$) and working-side ($p_{WS\text{-}max}$) condyles at HA_{maxRot}, respectively. Mean HA locations during the opening phase of the gape cycle are represented by red symbols and during the closing phase by blue symbols. Error bars correspond to the standard deviations in vertical and horizontal directions. The inset graph for each individual shows the mean Euler angle rotations around the X-, Y-, and Z-axis (indicated by blue, red, and green lines, respectively) from the reference position through the standardized gape cycle for right chews; grey boxes in the insets indicate the jaw closing phases of the gape cycle. Because Euler angle rotations are different for left and right chews, the X- and Z- Euler rotations of left chews were inverted to make the patterns through the gape cycle comparable. Thus, insets represent an average right chew cycle, using data from left and right chews.

correlations between the HA and gape angle. For *Cebus*, all individuals showed biologically relevant correlations between the horizontal position of the HA_{maxRot} and gape angle during both the opening and closing phases of the chew cycle. The vertical position of HA_{maxRot}, however, showed biologically relevant correlations with gape angle only for individuals C1 and C3 during the opening phase, and only for individual C3 during the closing phase. In *Macaca*, individual M2 only showed a biologically relevant correlation between the horizontal position of the HA_{maxRot} and gape angle during the closing phase of the chew cycle. Individual M3 showed biologically relevant correlations between both the vertical and horizontal position of the HA_{maxRot} with gape angle during both the opening and closing phases. Individual M2 showed no biologically relevant correlation.

3.2. Correlation between gonial angle and HA

The airway impingement hypothesis predicts a positive relationship between the horizontal projection of the mandible with respect to the mandibular condyle and the vertical position of the HA (HA_{vert}). Our findings do not indicate a significant relationship for the closing phase (Spearman's $\rho = 0.45$, $p = 0.26$) or the opening phase (Spearman's $\rho = -0.02$, $p = 0.95$). Overall, HA_{vert} was fairly constant, around 15% to 25% of jaw length below the TMJ, with the exception of one *Cebus* (individual C1) that had a higher HA located at around 10% of jaw length below the TMJ (Fig. 6).

3.3. Effect of HA position on the strain of the inferior alveolar neurovascular bundle (IANB)

The pattern of change in inter-foramina distance (IFD), our proxy for IANB strain, varied between species. IFD through the gape cycle for baboons and capuchins showed a very similar pattern, *decreasing* (i.e., shortening distance) until reaching maximum gape (Fig. 7). This decrease in distance was variable, from −2% in individual B1 to −12% in individual C1. This contrasts with the pattern observed in macaques where IFD *increased* through the gape cycle, reaching a maximum of 3% increase in distance in individuals M1 and M3. However, in the theoretical, simulated condition where the HA is at the TMJ, the IFD is expected to increase through the gape cycle reaching up to almost 4% strain in most individuals except C1 and C2. Thus, the difference

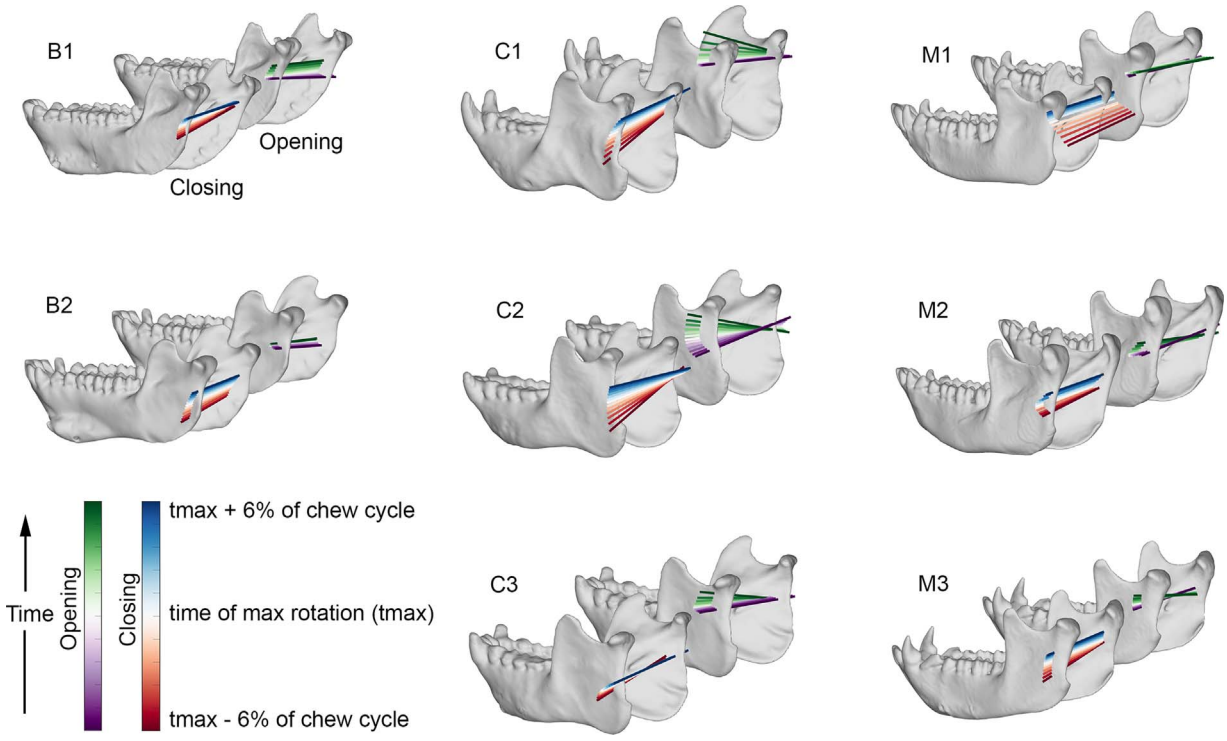

Fig. 4. Changes in the mean position and orientation of the helical axis (HA) during the opening and closing phases of the chewing cycles. Because chews on the left and right side have different patterns of HA orientation, orientations of HA from left chews were inverted around the sagittal plane, and all chews are represented as an average right chew. The different locations of the HA during the opening and closing phases of the gape cycle are represented by different colored lines: purple to green during the opening phase and red to blue during the closing phase. The timing of maximum rotation in both opening and closing phases is indicated by the white lines.

between the observed and simulated conditions shows that in most individuals (except for M1), a HA located away from the TMJ axis reduces to some degree the IANB strain.

3.4. Effect of HA position on muscle strain and moments

Muscle strain changes throughout the gape cycle and varies between individuals and species (Fig. 8). In general, muscle strain increases during the opening phase, reaching a peak at maximum gape, and then decreases during the closing phase. As expected, the posterior portions of each muscle are strained the least during the gape cycle, and in some cases, they even shorten (e.g., the posterior segment of the medial pterygoid in M3). On average, the medial pterygoid shows the least amount of strain and the masseter shows the greatest amount. In macaques, however, the temporalis shows similar or slightly greater strains than the masseter.

In the theoretical, simulated condition, where the axis of rotation passes through the TMJ, patterns of muscle strain were similar to those experimentally estimated, but with slight differences in their absolute magnitude. The differences between the observed and modeled muscle strains indicate that having a HA not passing through the jaw joints either maintains or reduces the muscle strains in both the medial pterygoid and masseter muscles, while *increasing* muscle strain in the temporalis (Fig. 8).

In all individuals, the moment arms of the anterior and middle portions of the medial pterygoid muscle are smaller than the corresponding parts of the masseter and temporalis muscles (Fig. 9). Throughout the gape cycle, posterior and intermediate muscle segments tend to decrease their moment arms until they reach maximum gape, while anterior segments either remain constant or increase their moment arms. In contrast, in a system where the TMJ functions as a hinge joint, in almost all muscle regions muscle moment arms decrease during jaw opening. This indicates that the actual location of the HA increases the moment arm of the muscles, especially the moment arm of the temporalis. The location of the HA in some cases increases the moment arm of the medial pterygoid (e.g., in capuchins) and in other cases that

Table 2
Correlation analyses of horizontal and vertical positions of the helical axis (HA) at maximum angular velocity (HA_{maxRot}) and maximum gape angle. Correlations with *r*-values > 0.3 are bolded.

Individual	Opening phase				Closing phase			
	HA horiz. position		HA vert. position		HA horiz. position		HA vert. position	
	r	*p*-value	*r*	*p*-value	*r*	*p*-value	*r*	*p*-value
B1	0.08	0.01	0.07	0.04	0.25	< 0.0001	0.00	0.80
B2	0.03	0.47	0.14	< 0.001	0.05	0.20	0.20	< 0.0001
C1	**0.36**	< **0.0001**	**0.40**	< **0.0001**	**0.46**	< **0.0001**	0.09	< 0.001
C2	**0.34**	< **0.0001**	0.08	< 0.01	**0.36**	< **0.0001**	–0.11	< 0.001
C3	**0.35**	< **0.0001**	**0.30**	< **0.0001**	**0.49**	< **0.0001**	**0.38**	< **0.0001**
M1	0.14	< 0.0001	0.19	< 0.0001	–0.17	< 0.0001	0.06	0.07
M2	0.18	< 0.001	0.06	0.24	**0.33**	< **0.0001**	–0.04	0.41
M3	**0.38**	< **0.0001**	**–0.60**	< **0.0001**	**0.59**	< **0.0001**	**–0.60**	< **0.0001**

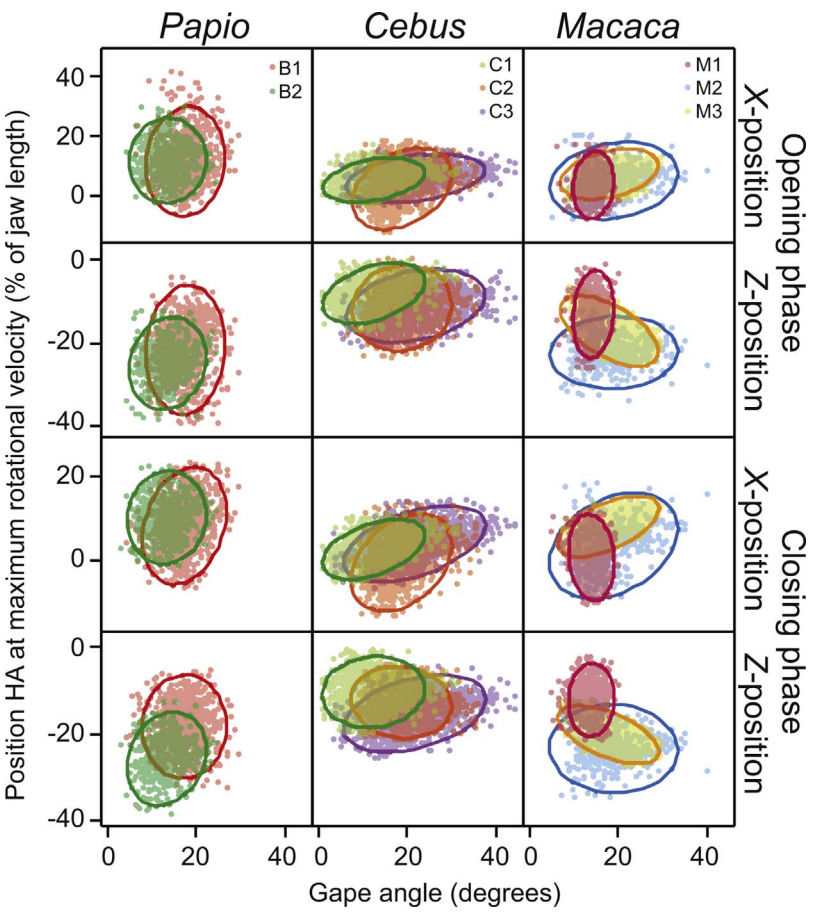

Fig. 5. Relationship between gape and the location of the helical axis (HA). Scatterplots between maximum gape angle and the horizontal (X-position) and vertical position (Z-position) of the HA_{maxRot}, for both opening and closing phases of the gape cycle. Within each plot, different colors represent different individuals. Individual correlations are depicted by 95% density ellipses, a graphical display of the correlation between two variables. These data correspond with the correlation results presented in Table 2.

of the masseter (e.g., in C2, C3, and M2).

Muscle moment arms around the moving HA ($M_{Muscle\text{-}HA}$) show a very different pattern (Fig. 10). First, because the HA becomes undefined at small angular velocities, we only present the data around the middle part of both the opening and closing phases of the gape cycle. There is a tendency for the moment arm to decrease during the opening phase and to increase during the closing phase, but this is variable among individuals. The difference between the observed moment arm around the HA and that around the theoretically simulated 'hinge-joint' condition shows that for the medial pterygoid and the masseter, this difference is small. For the medial pterygoid, anterior muscle segments tend to have higher differences in moments than more posterior segments. For the masseter, few differences in $\Delta M_{Muscle\text{-}HA}$ are noted between segments. The temporalis, however, shows higher differences in $\Delta M_{Muscle\text{-}HA}$ between segments, with more posterior fibers having higher differences between the observed moment and the simulated condition.

4. Discussion

4.1. 3D vs 2D estimates of AoR location

The obliquity of the rotational axis to the sagittal plane impacts the precision of estimates of the position of the AoR based on CoRs calculated from 2D image data (Carlson, 1977; Weijs et al., 1989; Terhune et al., 2011). Previously, we estimated the location of the AoR using lateral videofluoroscopy data collected in several taxa, including *Macaca* and *Cebus* (Terhune et al., 2011). The 3D data presented here allow us to assess the validity of our previous estimates of CoR location in *Macaca* and *Cebus* and discuss their implications for our estimates of CoR location in *Chlorocebus* and *Eulemur* (Terhune et al., 2011). The estimates of HA location in the current study were restricted to the times during jaw depression and elevation when rotational velocities were highest, corresponding roughly to the fast-open and fast-close phases of the gape cycle in Terhune et al. (2011). The results for *Cebus* presented in the present study show that the AoR is located anterior and inferior to the TMJ during fast open, moves posteriorly and inferiorly during fast close, and is located close to the level of the tooth row, corroborating Terhune et al. (2011). In contrast, the results for *Macaca* reported by Terhune et al. (2011) are not corroborated by the present study. Terhune et al. (2011) found highly variable AoR locations during fast open and fast close in macaques, mostly below the tooth row. The 3D results presented here show that in *Macaca* the AoR is located above or close to the level of the tooth row in all three individuals. The differences between these two studies could be explained by either methodological differences or intraspecific variation. The estimated position of the CoR (in 2D) is expected to be the average between the location of the AoR (in 3D) as it passes through the working- and balancing-side parasagittal planes, so differences in calculating the AoR in 2D vs. in 3D are unlikely to explain the differences between studies. A more likely explanation is that the timing at which the AoRs were calculated differs between these studies. In Terhune et al. (2011) the AoRs were calculated at different times throughout the different phases of the gape cycle. In our study, the mean AoR was estimated consistently as the mandible was moving with maximum angular velocity. As shown in Fig. 4, the location of the AoR moves inferior to superior through each of the phases. Thus, if the AoR were to be calculated in the earlier part of both the closing and opening phases, the location of the AoR would be lower. Finally, the subjects used in Terhune et al. (2011) are not the same as the ones used in this study, so it is possible that the observed differences between the studies could simply be due to intraspecific variability (see Section 4.2).

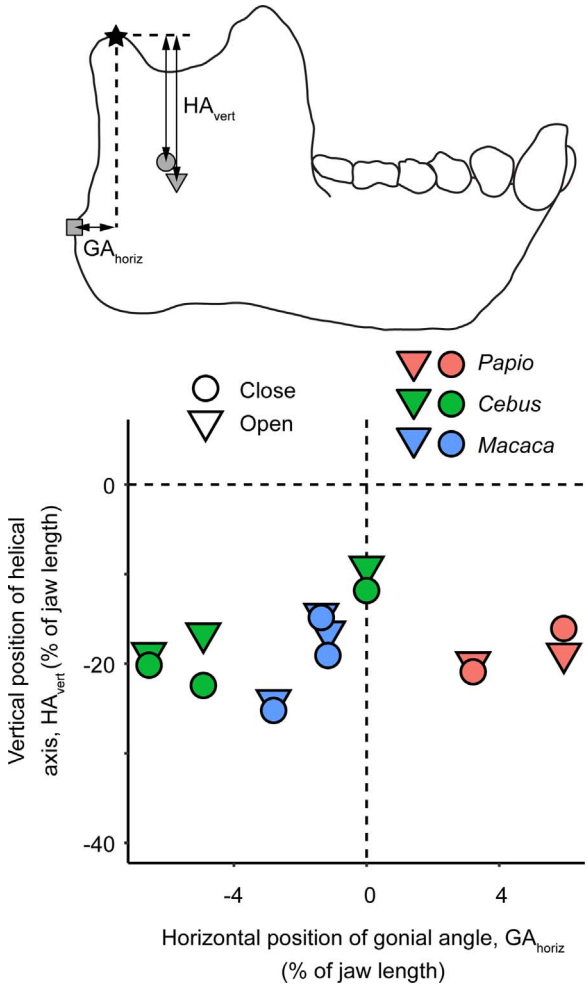

Fig. 6. Graph of the relationship between posterior protrusion of the gonial angle and mean helical axis position during chewing. The position of the most posterior point on the gonial angle (GA, grey square) and the mean helical axis (HA) for the opening and closing phases of the gape cycle (grey triangle and circle, respectively) were calculated relative to the top of the mandibular condyle (black star). The position of the HA was estimated as the intersection of the mean HA passing through the midline sagittal plane. In the plot below, circles and triangles represent the mean average for closing and opening phases of the gape cycle, and red, green and blue symbols represent the mean HA of *Papio*, *Cebus*, and *Macaca*, respectively.

4.2. Within- and between-species variation in AoR

Previous studies on non-human primates have shown substantial within-species variation in 3D kinematics (Iriarte-Diaz et al., 2011) and in masticatory muscle activation patterns (Vinyard et al., 2008). Here we show this variation is also reflected in the location and orientation of the AoR among individuals. Compared with *Papio*, *Cebus* and *Macaca* show more variability among individuals, both in terms of their AoRs at maximum angular velocity (Fig. 3) and in the way the AoR changes throughout the gape cycle (Fig. 4). The explanation for this intraspecific variation in the location and orientation of the AoR is not yet clear. Because of the potential effect that different AoRs could have on muscle and feeding mechanics, we would expect to also find some morphological differences among individuals. *Papio* mandibles are similar in shape, while *Cebus* and *Macaca* mandibles are more variable. For example, *Cebus* C1 has a relatively shorter mandibular corpus compared to that of C2, and *Macaca* M3 (the only male in our sample) has a relatively longer mandibular corpus compared to the other two individuals. Larger samples are needed to allow us to quantitatively assess the relationship between morphological variation and the AoR.

4.3. Functional significance of the AoR

4.3.1. The airway impingement hypothesis

Our data provide little support for the impingement hypothesis as an explanation for interspecific variation in HA location in non-human primates. If this hypothesis were correct, we would expect individuals with larger gonial angles to have more inferiorly located HAs than individuals with more obtuse mandibular angles. Across species, the mean vertical location of the AoR is relatively constant and it is not explained by gonial angle protrusion. Within species, there is an apparent trend wherein individuals with lower AoRs also have more protruded gonial angles, but our small samples and low statistical power do not allow for firm conclusions. In addition, if the impingement hypothesis were true, we would expect to see lower AoRs at larger gape angles, but there is little support for this hypothesis. The only biologically relevant negative correlation was found in the macaque M3, the only male in the study. Smith (1985) noted that an inferiorly positioned AoR is not a uniquely human trait, but also found in many other non-human mammals. He argued that although human airway structures are more vulnerable to impingement, this might also be a problem in non-human mammals, especially those that generate large gapes, such as *Papio* (Smith, 1985). The absence of a biologically relevant correlation in most of our individuals suggests that factors other than cervical impingement might drive the evolution of the AoR position in non-human mammals. Nonetheless, considering that inferiorly located AoRs are observed in many non-humans species, such as pigs,

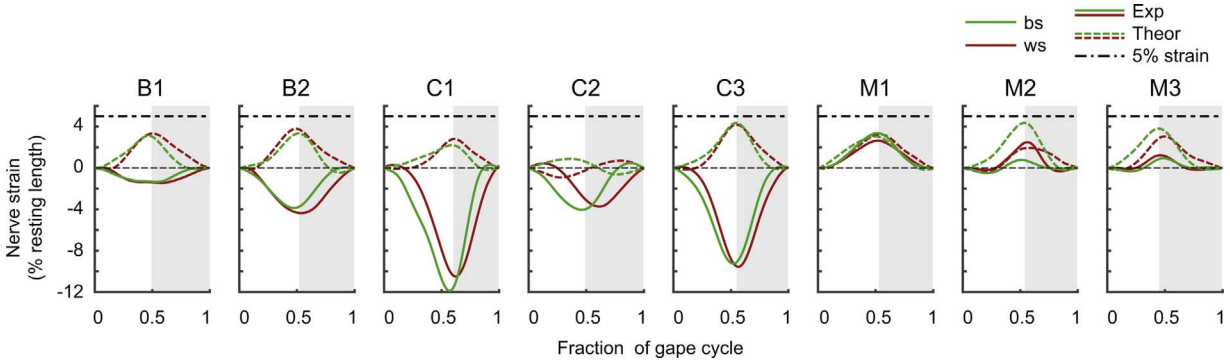

Fig. 7. Inferior alveolar neurovascular bundle (IANB) strain through the gape cycle in two baboons (B1, B2), three capuchins (C1, C2, C3), and three macaques (M1, M2, M3). Strain is estimated as the inter-foramen distance (IFD) between the foramen ovale and the mandibular foramen expressed as a percentage of the resting length–length at centric occlusion. Strain in the working-side (ws) nerve is represented by red lines and strain in the balancing-side (bs) nerve by green lines. Experimentally measured strains (Exp) are represented by solid lines and the simulated, hinge-joint data (Theor) by dashed lines at the top of the graphs. Grey bars indicate the jaw-closing phase of the gape cycle. Dashed lines represent a strain of 5% which has been shown to temporarily affect nerve conduction rate in Guinea pig nerve preparations (Rickett et al., 2011).

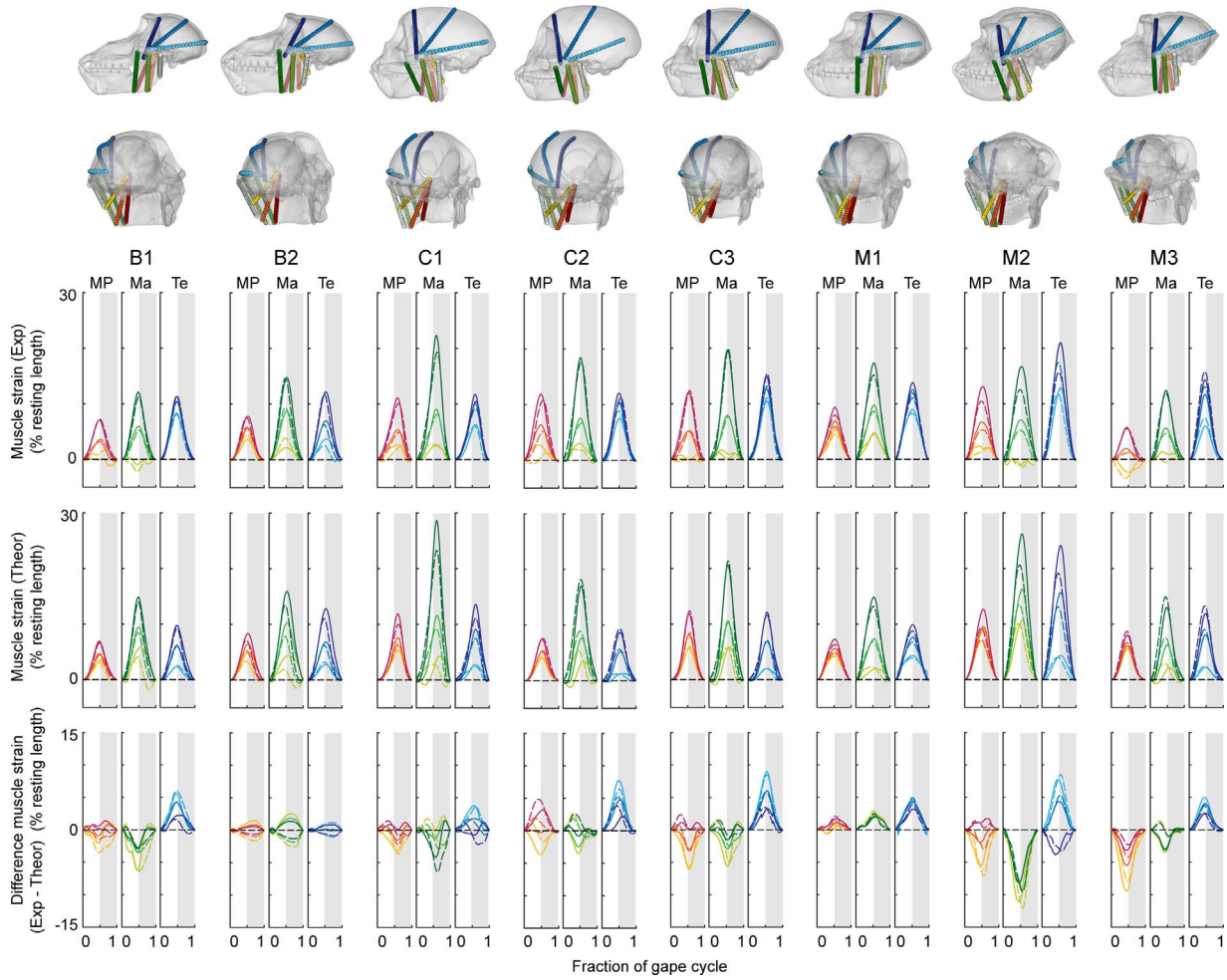

Fig. 8. Muscle strain − changes in total length as a percentage of resting length − of the major masticatory muscles throughout the standardized gape cycle for left chews in two baboons (B1, B2), three capuchins (C1, C2, C3), and three macaques (M1, M2, M3). The top row of figures shows the lines of action of the muscles in lateral view, the second row is from a posterior-lateral view to highlight the medial pterygoid. The colors of the traces match the segments of the muscles indicated in the diagrams at the top. Segments of the medial pterygoid (MP) are identified by shades of red; segments of the masseter (Ma) by shades of green; and segments of the temporalis (Te) by shades of blue. For each muscle, the anterior, middle and posterior segments are identified by dark, intermediate, and lighter colors, respectively. Muscles of the balancing and working side are indicated by solid and dashed lines, respectively. The plotted data are the experimentally observed data (Exp), the theoretical, hinge-joint condition data (Theor), and the difference between them (Exp − Theor). Grey bars indicate the jaw closing phase of the gape cycle.

rabbits, and other non-human primates (Weijs et al., 1989; Wall, 1999; Terhune et al., 2011; Menegaz et al., 2015), the AoR position in humans may be most parsimoniously interpreted as the retention of a primitive set of biomechanical features rather than a new functional trait.

4.3.2. Neurovascular hypothesis

If neurovascular strain were a major factor in determining the AoR location, ideally we would expect the bundle to undergo little strain, positive or negative, during normal feeding. The large amount of shortening that the IANB experiences at maximum gape in *Cebus* and *Papio*, and the small amount of nerve shortening in *Macaca*, suggests that the AoR location is determined by other factors and that nerve shortening is a by-product. In fact, the amount of strain on the IANB expected during normal feeding in the simulated hinge-joint condition does not exceed 5%, the minimal strain that has been observed to temporarily affect the conduction properties of peripheral nerves (Li and Shi, 2007; Rickett et al., 2011). It is worth mentioning that this 5% threshold is based on in vivo, acute experiments, and that it is possible that smaller strains could have some effects on the physiology of nerves under chronic, repetitive movements such as chewing. However, this is an unlikely scenario considering that, to our knowledge, no study has found a negative physiological consequence of low, cyclical strains on nerve physiology, and that many nerves that usually cross complex joints (e.g., shoulder, hip) are likely cyclically loaded at low strains during normal functioning. Thus, our data suggest that a pure hinge axis mandible movement does not produce biologically-relevant nerve strains and consequently that condylar translation is not needed to reduce IANB strain. Indeed, the fact that the theoretical (hinge-axis) condition approximates the AoR of many carnivores further suggests that IANB strain is not a relevant factor in determining AoR position.

4.3.3. Jaw-elevator torque hypothesis

The location of the AoR in our studied species effectively reduced the strains on the masseter/medial pterygoid complex with respect to a theoretical hinge joint. As the force output produced by muscle fibers is inversely proportional to the amount of strain once they are stretched beyond their optimal length, this decrease in strain would allow increased force output at wider jaw gapes (e.g., Eng et al., 2009). It is worth noting that the changes in muscle strain associated with variation in AoR location are maximal at or near maximum gape and decrease rapidly as the jaw approaches minimum gape. Mechanical benefits accruing to AoR location as pertain to force output will likely be obtained only during behaviors employing large gape distances. Thus, we can speculate that gape angle and AoR position should be correlated in species that actively generate wide jaw gapes during ingestive and biting behaviors, such as during tree gouging (Vinyard et al., 2003) or

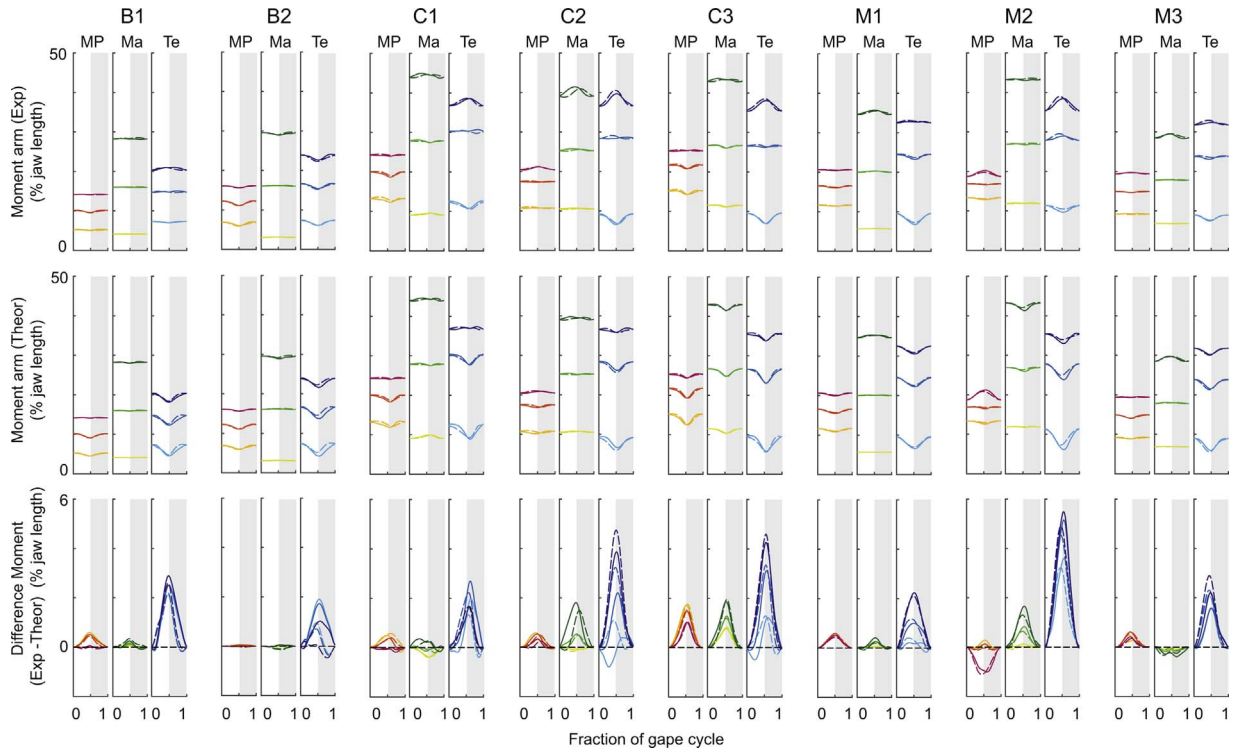

Fig. 9. Moment arm about the TMJ of the medial pterygoid (MP), masseter (Ma), and temporalis muscles (Te) over a standardized gape cycle in two baboons (B1, B2), three capuchins (C1, C2, C3), and three macaques (M1, M2, M3). Moment arm distances are presented as a percentage of jaw length. Segments of the MP are identified by shades of red; segments of the Ma by shades of green; and segments of the Te by shades of blue. For each muscle, the anterior, middle and posterior segments are identified by dark, intermediate, and lighter colors, respectively. Muscles of the balancing and working side are indicated by solid and dashed lines, respectively. The top panel shows the muscle moment arm calculated from the experimental data (Exp), the middle panel shows the moment arms of a theoretical, hinge-joint condition (Theor), and the bottom panel represents the difference in moment arm between the experimental and the theoretical data (Exp − Theor). Grey bars indicate the jaw closing phase of the gape cycle.

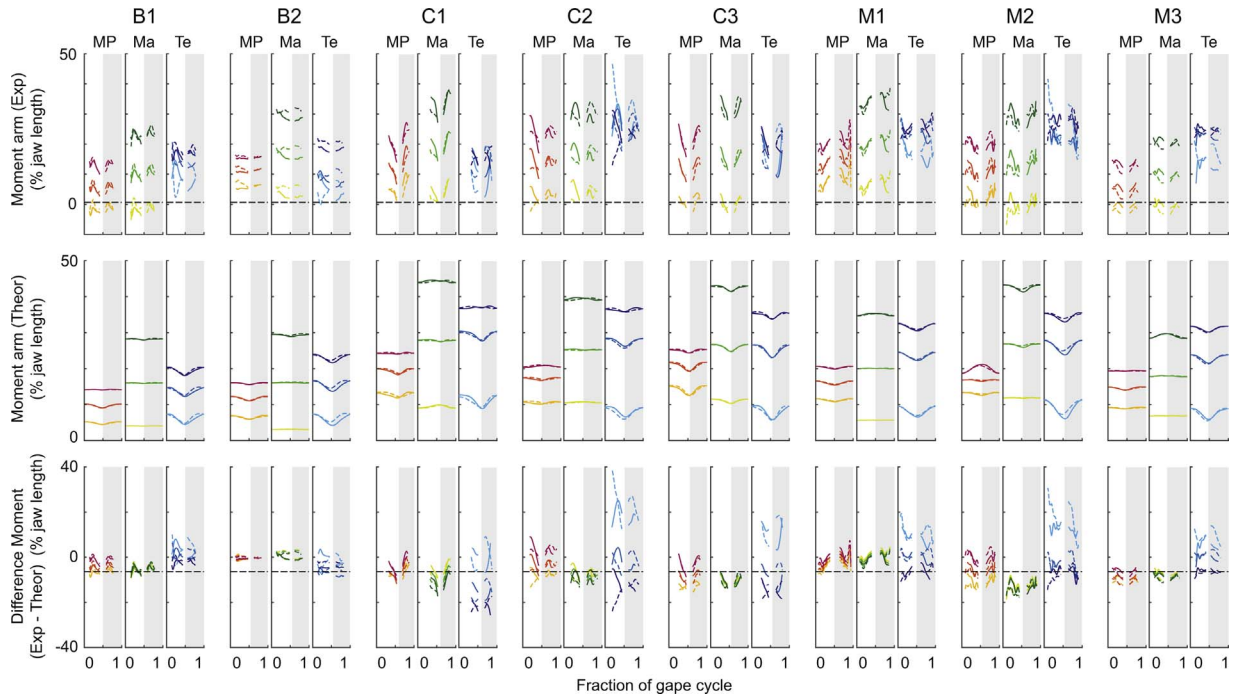

Fig. 10. Moment arm around the helical axis (HA) of the medial pterygoid (MP), masseter (Ma), and temporalis (Te) over a standardized gape cycle in two baboons (B1, B2), three capuchins (C1, C2, C3), and three macaques (M1, M2, M3). Distance data are presented as a percentage of jaw length. Segments of the MP are identified by shades of red; segments of the Ma by shades of green; and segments of the Te by shades of blue. For each muscle, the anterior, middle and posterior segments are identified by dark, intermediate, and lighter colors, respectively. Muscles of the balancing and working side are indicated by solid and dashed lines, respectively. Because the HA becomes undefined at low angular rotation velocities, calculations were only made for the data when HA rotation (ω) was greater than 10 degrees/sec. Grey bars indicate the jaw closing phase of the gape cycle. The top panel shows the muscle moment arm calculated from experimental data (Exp), the middle panel shows the moment arms of a theoretical, hinge-joint condition (Theor), and the bottom panel represents the difference in moment arm between experimental and theoretical data (Exp − Theor). Grey bars indicate the jaw closing phase of the gape cycle.

posterior molar biting of large, hard objects (Ross et al., 2016). The only individual that showed a biologically relevant correlation in the vertical position of the AoR was the single male in our sample, which showed large strain reduction in the posterior aspects of the masseter and medial pterygoid. Interestingly, all *Cebus* individuals showed a correlation between the horizontal position of the AoR and gape angle, especially during the closing phase, which also would bring the AoR closer to the masseter/medial pterygoid complex. This anteroposterior displacement of the AoR with gape angle might be important to compensate for the fact that in some cases, the position of the AoR moves closer to the condyle at higher gapes, contrary to expectations.

The way the position of the AoR affects the dynamics of muscle force generation is likely not straightforward. A single muscle can exhibit regional functional compartmentalization, either in terms of internal morphology or in activation patterns (see Higham and Biewener, 2011 for a general review). Morphological heterogeneity in non-primate mammals has been documented in complex, multipennate muscles such as the masseter (e.g., Nordstrom et al., 1974 − rats; Herring et al., 1979 − pigs; Weijs and Dantuma, 1981 − rabbits) but in primates there is limited information about regional morphological variation within masticatory muscles. In *Macaca fascicularis*, muscle fibers in the anterior portions of the masseter are longer than in posterior sections of the muscle (Terhune et al., 2015). These regional differences are functionally related to the amount of masseter muscle stretch, because longer fibers permit longer muscle excursion. However, for a given muscle volume, there is a trade-off between maximum muscle excursion and maximum force generation, such that longer muscle fibers allow for greater excursions but at some expense to muscle force (Gans and Bock, 1965). Shifting the AoR closer to the masseter/medial pterygoid complex is expected to reduce the need for increasing fiber length in the anterior muscle segments. The complex internal architecture of the jaw adductors makes it difficult to predict how differences in strain along the muscle influence different portions to produce force output. In addition to fiber architecture, passive effects on connective tissue elements in pinnate-fibered muscles may be responsible for altered muscle sarcomere dynamics (Azizi et al., 2008). Exploring dynamic changes in sarcomere length and orientation and their impact on whole muscle mechanics of the jaw adductors is an important next step in understanding the relationship between mandible kinematics and motor control.

In contrast to the masseter and the medial pterygoid muscles, muscle strains in the temporalis are increased with respect to the theoretical hinge-joint condition in all species, especially in the posterior portion of the muscle. This result could partially explain the unexpected finding by Terhune et al. (2015) that, contrary to the masseter, the shortest fibers in the *M. fascicularis* temporalis are located in the anterior parts of the muscle. In our sample, anterior temporalis fibers are stretched the most at high gape angles but the differences in strain between anterior and posterior fibers decrease with respect to the hinge-joint condition. Moving the AoR inferior to the TMJ joint would help maintain similar levels of stretch across the muscle at submaximal gapes, unlike what is observed in the masseter and medial pterygoid. These data suggest that anterior and posterior fibers of the temporalis can operate at similar points on the length–tension curve through large parts of the gape cycle, and that it could potentially generate consistent forces across the whole muscle. This in part supports previous arguments that the temporalis has evolved for a functionally different role from the masseter and medial pterygoid, with the temporalis being associated with producing large vertical occlusal forces during chewing (Hylander et al., 2005; Vinyard et al., 2007, 2008; Vinyard and Taylor, 2010)

4.4. Significance of AoR location for mandibular rotation and for bite force generation

The ability of the jaw-elevator muscles to generate *dynamic* jaw-elevating torques is affected by their position and orientation relative to the AoR, just as one's ability to open or close a door is affected by whether one pushes on the door close to the axis of rotation (the hinge) or further away from it. Stern (1974: p. 109) is correct that, as expressed by D'Alembert's principle, "if the muscle, joint, and reversed effective forces are all taken into account, the calculated acceleration will be independent of the point about which torques are *measured*" (emphasis added), but this does not obviate the fact that the same muscle force applied further from the AoR contributes more torque to rotation about that axis than the same force applied closer to it. Our data suggest that, compared with an AoR at the TMJ axis, the inferior location of the actual AoR improves the moment arm of the posterior temporalis muscle about the rotational axis, while the moment arms of the other muscles are not strongly affected.

The ability to produce torque in a static or quasi-static situation, such as during occlusion or biting, is influenced in part by the position and orientation of the AoR relative to the TMJ axis. As previously mentioned, the effect of shifting the location of the AoR is evident at large gapes but it decreases rapidly as the mandible approaches minimum gape. Our results indicate the moment arms of the temporalis, especially of the anterior segments of the muscle, are increased with respect to the hinge-joint condition, partially compensating for the increased strains that the muscle fibers experience. In *Cebus*, the moments around the TMJ axis of both masseter and medial pterygoid also increase with respect to the hinge-condition, suggesting that this may be particularly beneficial in species in which biting at relatively wide jaw gapes, such as posterior molar biting, is an important behavior.

4.5. Effect of gape angle on AoR location

Because only rhythmic chews were analyzed in this study, the range of gape angles observed here are expected to be smaller than the maximum gapes (and gape angles) these animals can generate. The limited range of gapes during feeding may account, in part, for the lack of a consistent correlation between gape angle and AoR. For example, we observed no correlation between gape angle and AoR in baboons (gapes limited to < 30 degrees in this study), while these same individuals produced much larger gapes (> 50 degrees) when they engaged in canine display during feeding sessions (Iriarte-Diaz, pers. obs.). Interestingly, the strongest correlation between location of the AoR and gape angle was observed in the only male (macaque M3) in our sample. The Rhesus macaque (*M. mulatta*), the macaque species used in the present study, is a highly dimorphic species and it has been shown that the masseter in males has a smaller mechanical advantage than that in females (Dechow and Carlson, 1990); this has been associated with an increased ability of males to produce large gapes. If large gapes are achieved at the expense of force generation, we can hypothesize that species that generate large gapes will have AoRs located at the level of the masseter/medial pterygoid complex and they will display a strong correlation between AoR location and gape angle, to alleviate the muscle length–force trade-off.

5. Conclusions

The location of the AoR of the mandible was calculated during feeding in eight individuals from three species of non-human primates to test hypotheses regarding the location of the HA and the functional significance of anteroposterior condylar translation in the TMJ during chewing. The mean locations of the HA at the times of maximum angular opening and closing velocity varied between individuals, but there are species-specific patterns in its vertical and anteroposterior position. There was little support for the impingement hypothesis between species, but some support within species. Contrary to expectations, species with larger gonial angles did not have more inferiorly located HAs. The neurovascular stretch hypothesis is not supported: the magnitudes of nerve strain that the animals would incur with the AoR

through the TMJs fall below the 5% strain that has been cited to produce conduction problems and well below the range at which conduction is irreversibly damaged. HA location has a greater effect on muscle moment arms about the TMJ, with implications for the torque generation capability of the jaw-elevator muscles. It is noteworthy that in *Cebus* the actual HA location is associated with larger jaw-elevator muscle moment arms about the TMJ than if the AoR were at the TMJ. Importantly, the effects of HA location on muscle strain and muscle moment arms are largest at large gapes and smallest at low gape distances, suggesting that if HA location is of any functional significance for primate feeding system performance, it is more likely to be in relation to large-gape feeding behaviors than chewing.

Acknowledgments

Christine Wall at Duke University kindly provided one of the animals used in this study; Dr. Charles Pelizzari at University of Chicago CT scanned the animals. We thank two anonymous reviewers for very thoughtful and helpful comments on the manuscript. This research was supported by NSF Physical Anthropology (NSF BCS 0240865) (to C.F.R., Co-PI), an NSF HOMINID grant (BCS 0725147) (to C.F.R., Co-PI), and the Brain Research Foundation of the University of Chicago (to C.F.R., Co-PI).

Appendix A. Supplementary data

Supplementary data associated with this article can be found, in the online version, at http://dx.doi.org/10.1016/j.zool.2017.08.006.

References

Anapol, F., Herring, S.W., 1989. Length–tension relationships of masseter and digastric muscles of miniature swine during ontogeny. J. Exp. Biol. 143, 1–16.
Azizi, E., Brainerd, E.L., Roberts, T.J., 2008. Variable gearing in pennate muscles. Proc. Natl. Acad. Sci. USA 105, 1745–1750.
Bennett, N.G., 1908. A contribution to the study of the movements of the mandible. Proc. R. Soc. Med. 1, 79–98.
Beyer, B., Sholukha, V., Salvia, P., Rooze, M., Feipel, V., Van Sint, S., 2015. Effect of anatomical landmark perturbation on mean helical axis parameters of in vivo upper costovertebral joints. J. Biomech. 48, 534–538.
Carlson, D.S., 1977. Condylar translation and the function of the superficial masseter muscle in the rhesus monkey (*M. mulatta*). Am. J. Phys. Anthropol. 47, 53–63.
Dechow, P.C., Carlson, D.S., 1990. Occlusal force and craniofacial biomechanics during growth in rhesus monkeys. Am. J. Phys. Anthropol. 83, 219–237.
Eng, C.M., Ward, S.R., Vinyard, C.J., Taylor, A.B., 2009. The morphology of the masticatory apparatus facilitates muscle force production at wide jaw gapes in tree-gouging common marmosets (*Callithrix jacchus*). J. Exp. Biol. 212, 4040–4055.
Farrar, W.B., 1978. Characteristics of the condylar path in internal derangements of the TMJ. J. Prosthet. Dent. 39, 319–323.
Gallo, L.M., Airoldi, G.B., Airoldi, R.L., Palla, S., 1997. Description of mandibular finite helical axis pathways in asymptomatic subjects. J. Dent. Res. 76, 704–713.
Gallo, L.M., Fushima, K., Palla, S., 2000. Mandibular helical axis pathways during mastication. J. Dent. Res. 79, 1566–1572.
Gallo, L.M., Brasi, M., Ernst, B., Palla, S., 2006. Relevance of mandibular helical axis analysis in functional and dysfunctional TMJs. J. Biomech. 39, 1716–1725.
Gans, C., Bock, W.J., 1965. The functional significance of muscle architecture: a theoretical analysis. Adv. Anatomy, Embryol. Cell Biol. 38, 115–142.
Grant, P.G., 1973a. Biomechanical significance of the instantaneous center of rotation: the human temporomandibular joint. J. Biomech. 6, 109–113.
Grant, P.G., 1973b. Lateral pterygoid: two muscles? Am. J. Anat. 138, 1–9.
Herring, S.W., Grimm, A.F., Grimm, B.R., 1979. Functional heterogeneity in a multipinnate muscle. Am. J. Anat. 154, 563–575.
Higham, T.E., Biewener, A.A., 2011. Functional and architectural complexity within and between muscles: regional variation and intermuscular force transmission. Phil. Trans. R. Soc. B 366, 1477–1487.
Hiiemäe, K.M., Kay, R.F., 1973. Evolutionary trends in the dynamics of primate mastication. In: Zingeser, M.R. (Ed.), Symposium Fourth International Congress of Primatology. vol. 3: Craniofacial Biology of Primates, Karger; Basel, pp. 28–64.
Hylander, W.L., 1975. The human mandible: lever or link? Am. J. Phys. Anthropol. 43, 227–242.
Hylander, W.L., 1978. Incisal bite force direction in humans and the functional significance of mammalian mandibular translation. Am. J. Phys. Anthropol. 48, 1–7.
Hylander, W.L., 2006. Functional anatomy and biomechanics of the masticatory apparatus. In: Laskins, D.M., Greene, C.S., Hylander, W.L. (Eds.), Temporomandibular Disorders: An Evidence Approach to Diagnosis and Treatment. Quintessence Publishing Co, New York, pp. 3–34.
Hylander, W.L., Wall, C.E., Vinyard, C.J., Ross, C., Ravosa, M.R., Williams, S.H., Johnson, K.R., 2005. Temporalis function in anthropoids and strepsirrhines: an EMG study. Am. J. Phys. Anthropol. 128, 35–56.
Iriarte-Diaz, J., Reed, D.A., Ross, C.F., 2011. Sources of variance in temporal and spatial aspects of jaw kinematics in two species of primates feeding on foods of different properties. Integr. Comp. Biol. 51, 307–319.
Katzberg, R.W., Keith, D.A., Guralnick, W.C., Ten Eick, W.R., 1982. Correlation of condylar mobility and arthrotomography in patients with internal derangements of the temporomandibular joint. Oral Surg. Oral Med. Oral Pathol. 54, 622–627.
Keefe, D.F., O'Brien, T.M., Baier, D.B., Gatesy, S.M., Brainerd, E.L., Laidlaw, D.H., 2008. Exploratory visualization of animal kinematics using instantaneous helical axes. Comput. Graph. Forum 27, 863–870.
Keefe, D.F., Ewert, M., Ribarsky, W., Chang, R., 2009. Interactive coordinated multiple-view visualization of biomechanical motion data. IEEE Trans. Vis. Comput. Graph. 15, 1383–1390.
Li, J., Shi, R., 2007. Stretch-induced nerve conduction deficits in guinea pig ex vivo nerve. J. Biomech. 40, 569–578.
Menegaz, R.A., Baier, D.B., Metzger, K.A., Herring, S.W., Brainerd, E.L., 2015. XROMM analysis of tooth occlusion and temporomandibular joint kinematics during feeding in juvenile miniature pigs. J. Exp. Biol. 218, 2573–2584.
Moss, M.L., 1960. Functional anatomy of the temporomandibular joint. In: Schwartz, L. (Ed.), Disorders of the Temporomandibular Joint. W. B. Saunders Co, Philadelphia, pp. 73–88.
Moss, M.L., 1975. A functional cranial analysis of centric relation. Dent. Clin. North Am. 19, 431–442.
Moss, M.L., 1983. The functional matrix concept and its relationship to temporomandibular joint dysfunction and treatment. Dent. Clin. North Am. 27, 445–455.
Nordstrom, S.H., Yemm, R., 1974. The relationship between jaw position and isometric active tension produced by direct stimulation of the rat masseter muscle. Arch. Oral Biol. 19, 353–359.
Nordstrom, S.H., Bishop, M., Yemm, R., 1974. The effect of jaw opening on the sarcomere length of the masseter and temporal muscles of the rat. Arch. Oral Biol. 19, 151–155.
Reed, D.A., Ross, C.F., 2010. The influence of food material properties on jaw kinematics in the primate, *Cebus*. Arch. Oral Biol. 55, 946–962.
Reinschmidt, C., van den Bogert, T., 1997. KineMat, A MATLAB Toolbox for Three-Dimensional Kinematic Analyses. University of Calgary, Calgary. http://isbweb.org/software/movanal/kinemat/index.html.
Rickett, T., Connell, S., Bastijanic, J., Hegde, S., Shi, R., 2011. Functional and mechanical evaluation of nerve stretch injury. J. Med. Syst. 35, 787–793.
Ross, C.F., Iriarte-Diaz, J., Reed, D.A., Stewart, T.A., Taylor, A.B., 2016. In vivo bone strain in the mandibular corpus of *Sapajus* during a range of oral food processing behaviors. J. Hum. Evol. 98, 36–65.
Smith, R.J., 1985. Functions of condylar translation in human mandibular movement. Am. J. Orthod. 88, 191–202.
Söderkvist, I., Wedin, P.Å., 1993. Determining the movements of the skeleton using well-configured markers. J. Biomech. 26, 1473–1477.
Stern, J.T., 1974. Biomechanical significance of the instantaneous center of rotation: the human temporomandibular joint. J. Biomech. 7, 109.
Terhune, C.E., Iriarte-Diaz, J., Taylor, A.B., Ross, C.F., 2011. The instantaneous center of rotation of the mandible in nonhuman primates. Integr. Comp. Biol. 51, 320–332.
Terhune, C.E., Hylander, W.L., Vinyard, C.J., Taylor, A.B., 2015. Jaw-muscle architecture and mandibular morphology influence relative maximum jaw gapes in the sexually dimorphic *Macaca fascicularis*. J. Hum. Evol. 82, 145–158.
Thexton, A.J., Hiiemae, K.M., 1975. The twitch-contraction characteristics of opossum jaw musculature. Arch. Oral Biol. 20, 743–748.
Van den Bogert, A.J., Reinschmidt, C., Lundberg, A., 2008. Helical axes of skeletal knee joint motion during running. J. Biomech. 41, 1632–1638.
Vinyard, C.J., Taylor, A.B., 2010. A preliminary analysis of the relationship between jaw-muscle architecture and jaw-muscle electromyography during chewing across primates. Anat. Rec. 293, 572–582.
Vinyard, C.J., Ravosa, M.J., Williams, S.H., Wall, C.E., Johnson, R., Hylander, W.L., 2007. Jaw-muscle function and the origin of primates. In: Ravosa, M.J., Dagosto, M. (Eds.), Primate Origins: Adaptations and Evolution. Springer, pp. 179–231.
Vinyard, C.J., Wall, C.E., Williams, S.H., Hylander, W.L., 2008. Patterns of variation across primates in jaw-muscle electromyography during mastication. Integr. Comp. Biol. 48, 294–311.
Wall, C.E., 1999. A model of temporomandibular joint function in anthropoid primates based on condylar movements during mastication. Am. J. Phys. Anthropol. 109, 67–88.
Weijs, W., Dantuma, R., 1981. Functional anatomy of the masticatory apparatus in the rabbit (*Oryctolagus cuniculus* L.). Netherlands J. Zool. 31, 99–147.
Weijs, W.A., Korfage, J.A.M., Langenbach, G.J., 1989. The functional significance of the position of the centre of rotation for jaw opening and closing in the rabbit. J. Anat. 162, 133–148.